Computer simulation of nonlinear interaction between a cold beam and a weakly collisional plasma

Hirotada Abe, Osamu Fukumasa, and Ryohei Itatani

Department of Electronics, Kyoto University, Kyoto 606, Japan

Hiroshi Naitou

Institute of Plasma Physics, Nagoya University, Nagoya 464, Japan
(Received 1 February 1978; final manuscript received 13 September 1978)

The spatial growth of the instability and the nonlinear interaction between a small cold beam and a warm background plasma are examined by means of particle simulation. Up to the first maximum in the amplitude oscillation of the wave, quantitative measurements confirm the predictions based on the single wave model: the magnitude of the growth rate, monochromaticity of the unstable mode, the maximum wave amplitude, and the phase space orbits of the beam electrons. After the first maximum of the wave amplitude, the spatial dependence of the wave amplitude cannot be explained by the single wave model predictions and the wave power is anomalously overdamped by a factor of 0.1 smaller than the predicted value in the first minimum. The extended single wave model equations suggest that this anomalous phenomenon is caused by weak collisions of the order of $\nu/\omega_p \sim 10^{-3}$ within the background plasma.

I. INTRODUCTION

The interaction between a beam and a plasma has been studied extensively since the beginning of research in plasmas. In nonlinear phenomena, the beam-plasma interactions have been investigated as a physical subject which has shown the essence of the nonlinearities most simply and typically. Theoretical and numerical studies[1–11] of the temporal and spatial evolutions in the cold beam and the plasma have been performed extensively within the last decade. Here, the adjectives, temporal and spatial, distinguish the differences in the boundary conditions: temporal means that the wave is periodic in space and grows in time from the initial value, whereas, spatial means that the wave is periodic in time and grows in space from the point where the beam enters the plasma. Their essential feature is the dominance of the most unstable mode in the system of the plasma and the cold beam. Drummond *et al.*[1] have shown that the most unstable wave develops linearly from the thermal fluctuation level, while the wave spectrum becomes progressively narrower. After several e foldings it becomes so narrow that a beam electron can detect a nearly pure sinusoidal wave or a single wave, and the wave grows to an amplitude sufficient to trap the beam.[1] It is different from the warm beam case to which quasi-linear theory can be applied.

By assuming that the beam electrons are interacting with the monochromatic and most unstable wave, and that the background plasma is a linear dielectric medium, both temporal and spatial single wave models are constructed. In these models, the phase space orbits of the beam electrons are numerically and self-consistently calculated. The electric field is calculated from the discrete beam charges and the continuum dielectric medium represented by the linear dispersion relation of the background plasma. O'Neil *et al.*[2,6] have shown that both descriptions of the temporal and spatial evolutions can be reduced to the same scaled equation in the infinitesimally small expansion parameter. In other words, there can exist an example such that the temporal and spatial problems are essentially equivalent even in the nonlinear regime. This result is similar to that of linear theory, in which we may predict the properties of the spatial evolution from those of the solution of the temporal evolution.

However, to what extent can we apply the single wave model predictions to real experiments? This problem has remained unsolved, although numerous experiments[12–17] have been performed concerning these beam-plasma interactions. Especially, experiments by Gentle and Lohr[13] revealed that the single wave model predictions were indeed correct through saturation and one amplitude oscillation bounce in the nonlinear regime. After that point, the experiments did not agree with the prediction.

The particle simulations of the temporal case have been performed by some authors.[18,19] Kainer *et al.*[19] have indicated that the initial growth of the unstable wave can be described by the two-stream instability and that the subsequent phenomena can be separated into two regions (high and low density), depending on whether or not merging of space-averaged velocity distributions occurs during the growth of the initially most unstable wave. However, we cannot apply these results directly to the spatial case, which we have usually treated experimentally, since the basic equations describing the spatial evolution do not become coincident with those of the temporal evolution in the expansion parameter of the finite value even within the framework of the single wave model.[11]

Shapiro and Shevchenko[7] have suggested that the condition for neglecting the nonlinearity of the plasma oscillation in the spatial evolution is very rigid and takes the form

$$\left(\frac{n_b}{n_p}\right)^{1/3} \ll \frac{v_g}{v_p} \cong 3\frac{v_t^2}{v_b^2}, \tag{1}$$

 0031-9171/79/020310-11$00.90

where n_b and n_p are the beam and plasma densities, v_g is the group velocity of the unstable wave, and v_t and v_b are the plasma-thermal and beam-drift velocities.

The considerations concerning these problems have motivated us to develop a particle simulation model[20] treating the phenomena of plasma in the semi-infinite space approximately, in order to study the spatial evolution of the beam-plasma interaction and predict the experimental results. In addition, it would be possible to apply this technique to other problems of the wave such as lower hybrid wave propagation in a nonuniform density.[21]

As the simulation model treating the phenomena of the beam-plasma system in the semi-infinite space, we have substituted a model which can simulate plasmas in a finite system bounded by a pair of the metallic walls with the beam injectors in the left wall. When we try to approximate the semi-infinite plasma with the bounded plasma, we should consider the effects of the right wall on the beam-plasma interactions, except for the case that the distance between the walls is infinite. These effects may cause the reflection of the wave or the production of the standing wave. However, we found that the effects can be neglected if we can handle the system including more than ten wavelengths. The details are explained in Sec. III. In Sec. II, we abbreviate the single wave model predictions for comparison with simulation results and make a comparison between the predictions of the single wave model and those obtained from the more exact single wave model equations,[11] which include the effects of the weak collision and the finite expansion parameter. In Sec. V, we will discuss the comparison of our results with existing simulations, the theoretical and numerical work, and the experiments.

II. SINGLE WAVE MODEL PREDICTIONS IN THE SPATIAL EVOLUTION

A feature of the single wave model is that the basic equations describing the nonlinear interactions in the system of a cold beam and a warm plasma can be written by the universal variables which do not only depend on the basic parameters of the problem (i.e., n_p, n_b, v_t, and v_b), but also include all their dependences.[6] In other words, the scaled equations[6] which are derived from the single wave model equations by using the universal variables are the unique nonlinear equations, which do not depend on any basic parameters directly. This elegant model was obtained at a slight sacrifice of strictness. Actually, this model can be extended to be exact to higher orders of the expansion and to include collisional effects[11] and many wave effects,[10] at the sacrifice of the uniqueness of the scaled equations.

The scaling law[6] derived from the properties of the uniqueness of the scaled equations is an important feature in these beam-plasma interactions. For the purpose of understanding the qualitative properties of these beam-plasma interactions and of approximately estimating the characteristic quantities, the single wave model equations[6] are very satisfactory. The linear growth rate, the saturation level of the wave amplitude, and the length of the amplitude oscillation can be calculated from the scaled equations and the scaling law. Here, we present a summary of the fundamental results of the calculation[6] and these results will be compared with our simulation results.

In order to represent the scaling law, we introduce an expansion parameter κ which should be much less than unity

$$\kappa = \left(\frac{1}{6}\frac{n_b}{n_p}\frac{v_b^2}{v_t^2}\right)^{1/3} \ll 1 . \tag{2}$$

Then, the equations for the single wave model in the lowest order of κ give the universally scaled equations or Eqs. (12) in Ref. 6.

In the linear region where the instability develops from thermal fluctuations, only one mode with the maximum growth rate grows strongly after several e foldings. The frequency ω_{pt}, the wavenumber k, and the spatial growth rate γ are

$$\omega_{pt} = \omega_p[1 + 3(v_t^2/v_b^2)]^{1/2} , \tag{3}$$

$$k = k_0(1 + \kappa/2) , \tag{4}$$

$$\gamma = [(3)^{1/2}/2]\kappa k_0 , \tag{5}$$

where $\omega_p = (n_p e^2/\epsilon_0 m)^{1/2}$ and $k_0 = \omega_{pt}/v_b$.

At the point where the wave amplitude saturates after the linear growth or at the first maximum of the wave amplitude, the magnitude of the electric field and the bounce frequency of the trapped particle in the wave trough are

$$E_{\max} \cong 1.2\kappa^2(m/e)v_b^2 k_0 , \tag{6}$$

$$\omega_b \cong (1.2)^{1/2}\kappa\omega_p . \tag{7}$$

In the nonlinear region, where the wave amplitudes make the undamped but not growing oscillation, the period of its oscillation λ_A and the ratio r_E of the maximum wave energy to the minimum are the most characteristic quantities

$$\lambda_A \cong 5/\kappa k_0 , \tag{8}$$

$$r_E = E_{\max}^2/E_{\min}^2 \cong 5 . \tag{9}$$

Then, the maximum velocity $v_{b\max}$ and the minimum velocity $v_{b\min}$ of the trapped beam electrons are related to the phase velocity v_{ph} and the maximum of the electric field as follows[18,19]:

$$v_{ph} \cong v_b(1 - \kappa/2) ; \tag{10}$$

$$v_{b\max} - v_{ph} \cong v_{ph} - v_{b\min} \cong \Delta v , \tag{11}$$

$$\Delta v \cong \left(\frac{4e}{m}\frac{E_{\max}}{k_0}\right)^{1/2} \cong 2.2\kappa v_b . \tag{12}$$

III. SIMULATION MODEL

The simulation model adopted in this work is intended to be representative of some[12-17] of the beam-plasma systems in a sufficiently strong magnetic field having one-dimensional electron dynamics. This one-dimensional, electrostatic system of length L is bounded by a pair of conducting walls where the electrostatic potentials ϕ are zeros. For the method of calculating the interparticle forces, the cloud-in-cell model of Gaussian

clouds[22] is used. The potential ϕ is calculated by the expansion of the eigenmodes $[\sin(n\pi x/L); n=1, 2, \ldots, M]$,[23] using the method of fast Fourier transforms. The algorithm for advancing particles is the standard time-centered leap-frog scheme.[22]

This system contains the background and beam electrons immersed in immobile, uniform background ions. In order to reduce unacceptable statistical fluctuations owing to too few beam particles, the model can include both heavy and light particles, which are assigned to the background and beam electrons, respectively. The ratio e/m is the same for both types of particles in order to keep the acceleration due to the electric field the same.[19] Each beam electron with velocity v_b enters the system steadily from the left side ($x=0$). The beam electrons reaching the right wall are removed from the system. The background electrons reaching the walls are reflected with the same velocity but opposite sign on arrival.

The initial conditions of the particle distributions are described as follows; both the beam and background electrons are uniformly located in space, respectively. The background ion density is constant in time and is determined as the system is initially neutral. From the condition imposed on the motion of the particles, it is clear that the number of background electrons is constant in time, while the number of beam electrons is variable. This means that the system can be non-neutral. In this work, however, the ratios for non-neutrality were very small, because the beam densities were much smaller than the background densities and, in addition, the beam electrons were initially located uniformly in space. Therefore, this weak non-neutrality is of the order of the beam density fluctuation and scarcely changes the behavior of the beam-plasma interaction. The reason why we discarded the neutrality condition is the following: At first, we attempted to change the density of the background ions in time in order to satisfy the neutrality condition. Then, the density of the ions changed with frequency near one of the unstable modes. It excited a mode with a half-wavelength equal to the system size and changed the interactions in the beam-plasma systems considerably.

Both the initially located and the steadily injected beams are assumed to have drift velocity v_d. The initial velocities of the background electrons are selected at random from the Maxwellian distributions and adjusted for the thermal and drift velocities to equal v_t and zero, respectively, in each region of length $\Delta_v = L/N_v$, which is located from $x=(n-1)\Delta_v$ to $x=n\Delta_v$ $(n=1, 2, \ldots, N_v)$; N_v is 200 throughout this work.

We choose the simulation parameters as follows; the numbers of the beam and background electrons are 4000 and 80 000, respectively. The beam velocity v_b is $0.0114\ L\omega_p$: the transit time of the beam electrons through the system is about 90 ω_p^{-1}. With the grid separation Δ, the characteristic length can be represented: $L=2048\Delta$ $(M=2048)$, $R=3.5\Delta$, $\lambda_D=1.63\Delta\sim3.26\Delta$, $\lambda \cong 120\Delta\sim140\Delta$, where R is the cloud radius, λ_D is the Debye length, and λ is the wavelength of the unstable mode.

TABLE I. Simulation parameters.

	κ	n_b/n_p	v_b/v_t	v_b $(L\omega_p/2\pi)$	v_t $(L\omega_p/2\pi)$	$n\lambda_D$	Final time (ω_p^{-1})
Run E1	0.25	0.001	9.9	0.07	0.0071	90	552.0
Run E2	0.20	0.001	7.0	0.07	0.01	127	301.6
Run E3	0.20	0.0005	9.9	0.07	0.0071	90	674.3
Run E4	0.40	0.002	14.0	0.07	0.005	64	672.0

In the system which contains 15 to 17 wavelengths, the effects of the right conducting wall can be neglected for the fundamental wave-particle interactions except near the right wall, or it can be said that the system is semi-infinite (we confirmed that these systems can represent traveling waves, if they have more than 5 to 6 wavelengths and if the waves are not reflected at the right walls, as in the case treated here and in Ref. 21).

In these systems, the system cannot reach the fully steady state, because the temperature of the background electrons continues to increase gradually by obtaining a part of the beam energy through the wave. In addition, the computer time permitted for this work forced us to interupt the simulation runs, when we judged that it reached an approximately steady state.

Through all simulation runs, energy conservation[23] was better than 0.2%.

IV. RESULTS OF PARTICLE SIMULATION

Runs E1 to E4 were performed with the parameters shown in Table I. We adjusted the ratios n_b/n_p and v_b/v_t, such that the expansion parameters κ are 0.25 for E1, 0.2 for E2 and E3, and 0.4 for E4. From Eqs. (10)–(12), these parameters are expected to have the following features in phase space: The distributions of the trapped beam electrons are separated from those of the background electrons for $\kappa=0.2$, and are merged with those of the background electrons slightly and are merged deeply for $\kappa=0.25$ and $\kappa=0.4$, respectively.

At first, we present the details of the evolution in run E1, which is a typical one. Because the beam electrons are distributed uniformly in space at $t=0$, the initial growth of an unstable mode and the corresponding weak perturbation of the beam distribution occur everywhere in the system. In other words, the system evolves temporally[2] in the early stage of the run. As the unstable mode grows, the wave amplitude begins to grow spatially[6] as well as temporally and becomes largest at the right wall, near which the beam electrons are trapped. Then, the first maximum of the wave amplitude appears. The position of the maximum shifts to the left side and the magnitude of the maximum grows. Next, the first minimum of the wave amplitude appears, then the second maximum is observed, and so on. During that time, the observed growth rate in the linear stage gradually increases. In this way, the system reaches an almost stationary state.

Figures 1(a) and (b) present a spatial wave pattern at $t=360\ \omega_p^{-1}$ and a spatial dependence of the wave power averaged during 330 to 360 ω_p^{-1}, in which the system is

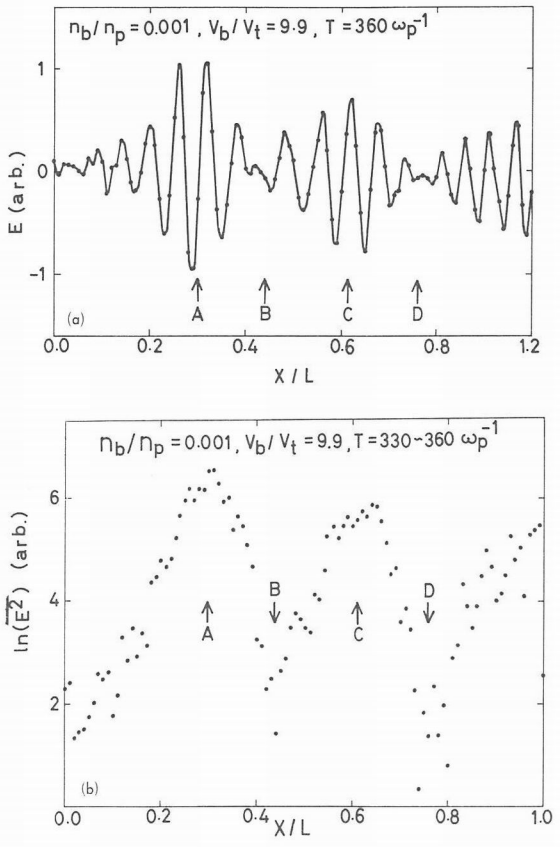

FIG. 1. The spatial dependences of the electric field before arrival at the stationary state for run E1: (a) An instantaneous wave pattern as a function of distance x from the beam injection. (b) The spatial dependence of the average wave power as a function of distance x. The ratio of the first maximum of the wave power to the first minimum is about 50, which is larger by a factor of about 10 than the value $r_E \sim 5$ in Eq. (9).

in a transient state. They show three amplitude oscillations of the wave. The most unstable mode grows from the thermal fluctuation and saturates at a point A, where the wave amplitude is the first maximum. After A, the wave amplitude oscillates in space to become the first minimum at B, the second maximum at C, and the second minimum at D. It is most characteristic that the minimum wave power damps by a factor of about 0.1 smaller than that expected from the prediction of the single wave model.[6] During this time the system does not reach the stationary state sufficiently. Even if the system approaches the stationary state, the overdamping of the minimum amplitude was also observed (Fig. 3). The phenomenon of overdamping will be discussed in detail for the example of run E3.

Figure 2 shows the instantaneous phase space plot at $t = 345.6\ \omega_p^{-1}$. The beam electrons which enter from the left wall undergo velocity modulation, as the wave grows exponentially in space. Next, the phase space loci of the beam electrons become curved strongly and begin to rotate in phase space, when the wave grows large enough to trap the beam electrons. O'Neil *et al.*[2,6] showed that this rotation was caused by the sloshing back and forth in the wave trough. Figure 2 suggests the following: The beam velocity decreases strongly at point A, where the wave amplitude is a maximum. Then, the beam electrons are accelerated by the wave and form a hollow vortex in phase space after A, while the wave amplitude decreases and becomes a minimum at B. These appearances correspond to the prediction of the single wave model[6] exactly. In the next stage after B, the appearance of the phase space loci does not become coincident with the prediction in accordance with the overdamping of the minimum wave amplitude at B. Namely, the faster beam and slower beam electrons near B can be insufficiently decelerated and accelerated, respectively, for the phase space loci of the beam electrons to agree with the prediction,[6] because the wave amplitude is very small at B. As a result, the hollow vortex of the beam in phase space becomes inclined after B. The beam electrons seem to be instantaneously detrapped from the wave trough. As the beam electron approaches point C of the second maximum of the wave amplitude, the inclined vortex begins to undergo a

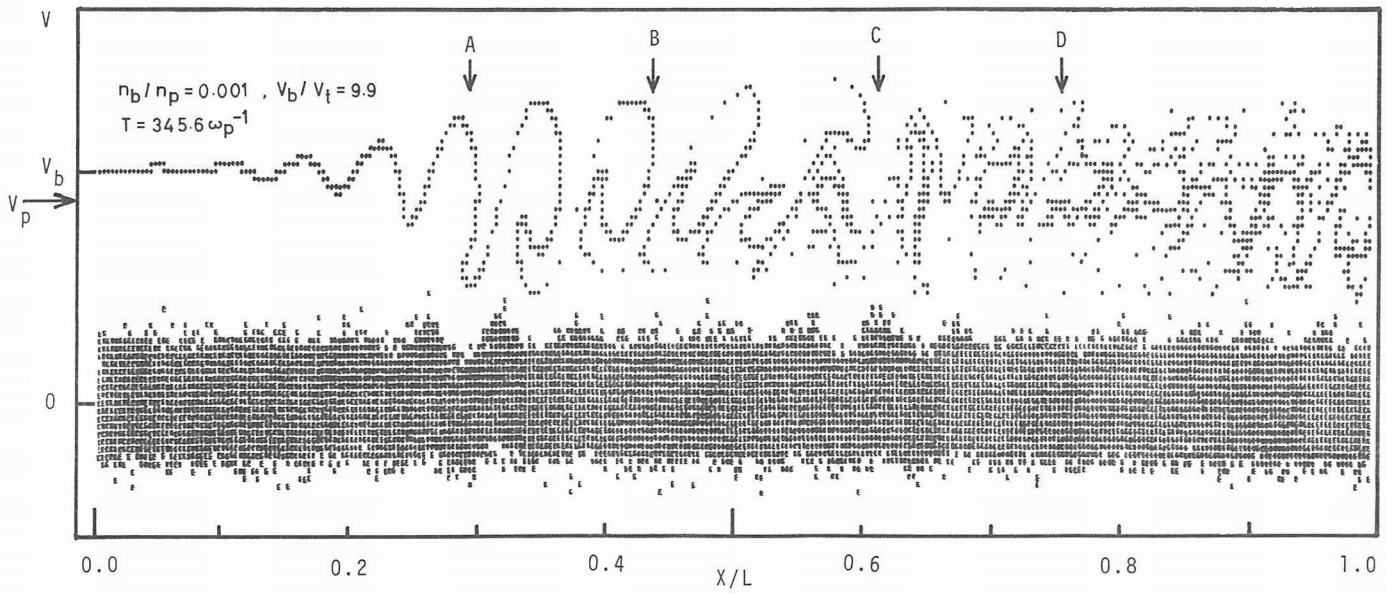

FIG. 2. The instantaneous phase space plot at the time corresponding to that in Fig. 1 for run E1. Four arrows indicated by the symbols A, B, C, and D indicate the characteristic positions from the first maximum to the second minimum as shown in Fig. 1. The value V_p is the theoretical phase velocity calculated from Eq. (10).

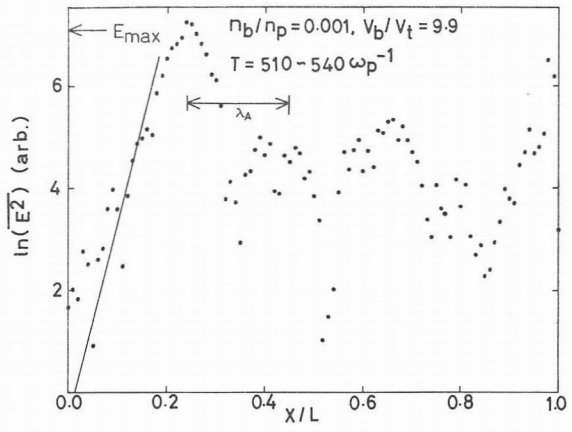

FIG. 3. The spatial dependence of the wave power in the stationary state for run E1. The solid line corresponds to the theoretical linear growth. The values designated by the symbols E_{max} and λ_A are the maximum of the wave power and the wavelength of the amplitude oscillation predicted by the single wave model.

strong effect of the wave and the insufficiently decelerated beam electrons at the upper part in phase space plane are again trapped to be a new vortex and overtake the insufficiently accelerated beam vortex. Namely, the slow vortex seems to shoulder the fast vortex. As a result, the vortex is split into two vortices. At point C of the second maximum of the wave amplitude, these two vortices mix and lose their original form. Although this behavior was observed in the transient state, the features were not changed in the stationary state (Fig. 5).

About 200 ω_p^{-1} later from the time shown in Fig. 1, the system reaches the almost stationary state. As shown in Fig. 3, which presents a spatial dependence of the wave power, the measured growth rate agrees with the value calculated from linear theory or Eq. (5), and the amplitude of the electric field at the first maximum is close to the value calculated from Eq. (6). After the first minimum, however, the appearance of the spatial evolution of the electric field departs from the predictions.[6] Namely, it fails to recover the amplitude nearest to the first maximum. This feature is in contrast to the previous one and can be called the destruction of the amplitude oscillation.[17] In Figs. 4(a) and (b), we show the spatial dependence of the frequency spectra and of the most dominant mode and its side band modes up to the second minimum. It shows the dominance of the single mode in accordance with the prediction.[1,2,6] However, its frequency $\omega = 1.047\ \omega_p$, is larger than the frequency $\omega_{pt} = 1.015\ \omega_p$, which is that of the theoretically most unstable mode, calculated from Eq. (3). A part of its origin may be due to the nonlinear effects of the beam electrons, as discussed in Sec. V. As pointed out by O'Neil *et al.*,[2,6] the secondary harmonics is observed near the first maximum. At the first minimum, the peak of the spectrum seems to shift by about $0.05\ \omega_p$ to the higher frequency side as a result of the overdamping of the most dominant mode.

Figure 5 shows the instantaneous phase space plot at $t = 518.4\ \omega_p^{-1}$. Let us compare this with the phase space plot in Fig. 2, which was observed at about 200 ω_p^{-1} before this time, namely, at 345.6 ω_p^{-1}. The maximum electric field grows larger than that at the previous time [compare Figs. 1(b) and (3)]. Therefore, the beam electrons are decelerated by the wave more strongly than before and are merged with the background electrons near the point of the maximum electric field [compare those in Figs. (2) and (5)]. It is noted that the destruction of the amplitude oscillation seen in Fig. 3 occurred at almost the same time in growth of this merging, although it is unclear whether it causes the destruction or not. The spreading of the beam velocity agrees with the value, $2\Delta v$, calculated from Eqs. (11) and (12).

Figures 6 and 7 show the spatial dependence of the wave power in the case of runs E2 and E3 with the same expansion parameter of $\kappa = 0.2$ and with different plasma parameters $n_b/n_p = 0.001$, $v_b/v_t = 7$, and $n_b/n_p = 0.0005$, $v_b/v_t = 9.9$, respectively. In the limit of small κ, these two runs should have the same stationary state. In the transient state, the systems evolve temporally at first, and begin to form the spatial evolution with the temporal saturation. Therefore, it is observed that run E2 has grown faster than run E3, because of the larger temporal expansion parameter[2] $(\frac{1}{2}n_b/n_p)^{1/3}$, which corresponds to κ in the spatial case. From the linearly growing region to the second maximum, both spatial variations of the

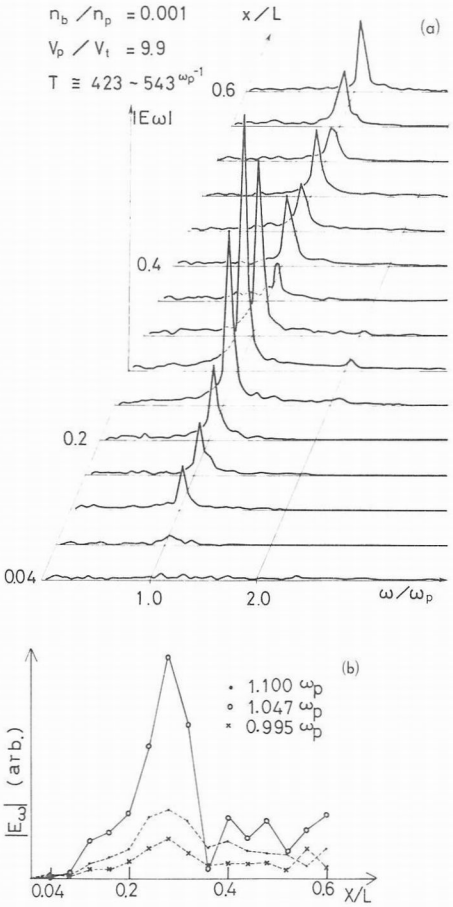

FIG. 4. The frequency spectra for run E1: (a) The spatial dependence of the spectra between $t = 423\ \omega_p^{-1}$ and $543\ \omega_p^{-1}$. The minimum frequency separation is $0.052\ \omega_p$. (b) The spatial dependences of the most dominant mode and its side band modes.

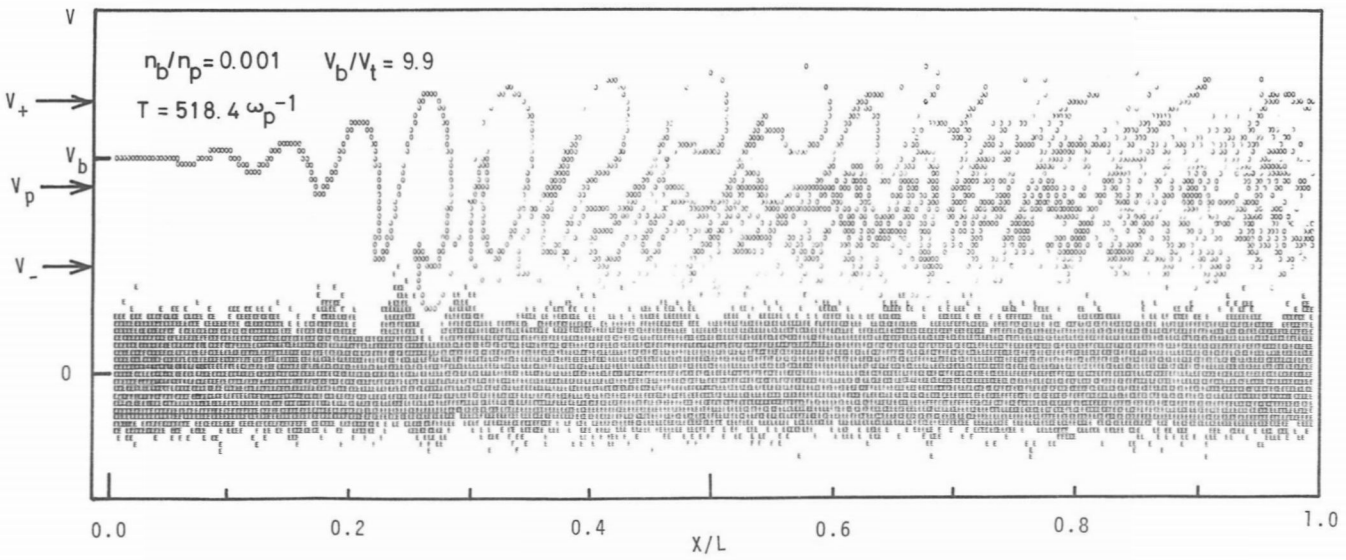

FIG. 5. The instantaneous phase space plot in the stationary state. The value V_p is the theoretical phase velocity, v_{ph}, and V_- and V_+ are $v_{ph} - 2^{-1/2}\,\Delta v$ and $v_{ph} + 2^{-1/2}\,\Delta v$, where v_{ph} and Δv are given in Eqs. (10) and (12) (run E1).

wave powers in runs E2 and E3 resemble each other, but begin to depart after the second maximum. Figure 8 shows the instantaneous phase space plot of run E3. In this case, the beam electrons are separated slightly from the background electrons, and the nonlinearities associated with the background electrons are expected to be weaker than those in runs E1 and E4. However, we should usually take account of the weak collisional effects, which may play an important role in the nonlinear stage. Therefore, we have extended the single wave model equations to the more rigorous ones[11] including collisional effects between the plasma electrons, and the higher order effects of κ. Typical results are shown in Figs. 9 and 10. The value η shown in the figures is the normalized distance $\eta = \kappa k_0 x$. The dashed and solid curves show the wave powers as a function of the distance η from the beam injection in the collisionless and slightly collisional cases, respectively. Some other plasma parameters are chosen to fit those in run E3 for comparison.

In spite of the very large κ ($\kappa = 0.2$), the collisionless case scarcely changes its qualitative features compared with the case[6] for $\kappa = 0$, while the collisional case shows an interesting change: Before $\eta = 11$ or the point of the first maximum of the wave amplitude, the collisional effect does not significantly alter the spatial evolution of the wave except that the wave amplitude saturates at a slightly lower level than that in the collisionless case, as shown in Fig. 9. After this point, however, the two curves begin to depart from each other. Near the first minimum, the wave amplitude decreases drastically, becomes much smaller than that in the collisionless case, and fails to regrow to the initial saturation level in the second maximum. These features closely resemble those in run E3. Here, we estimate the effective collision frequency ν in run E3: the collision frequency ν of the one-dimensional particle simulation has the relationship[24,25] with the plasma density n_p and the Debye length λ_D, i.e., $\omega_p \nu^{-1} = \alpha (n_p \lambda_D)^2$, where α is a numerical factor and is about 0.1 in the model adopted here, and $n_p \lambda_D \cong 90$ in run E3. Therefore, the calculated value of ν/ω_p is about 1.2×10^{-3}, which is comparable to the value $\nu/\omega_p = 2 \times 10^{-3}$, shown in Figs. 9 and 10. Now, we can conclude that the origin of the overdamping of the first minimum is due to a weak collision of the order of 10^{-3}, which scarcely changes the linear growth and the saturation level in the first maximum of the wave amplitude.

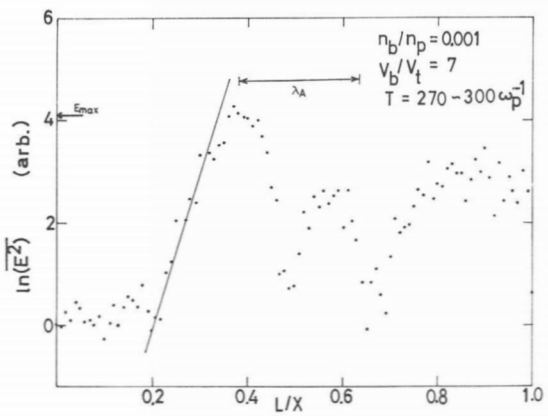

FIG. 6. The spatial dependence of the average wave power between $t = 270\ \omega_p^{-1}$ and $300\ \omega_p^{-1}$ (run E2).

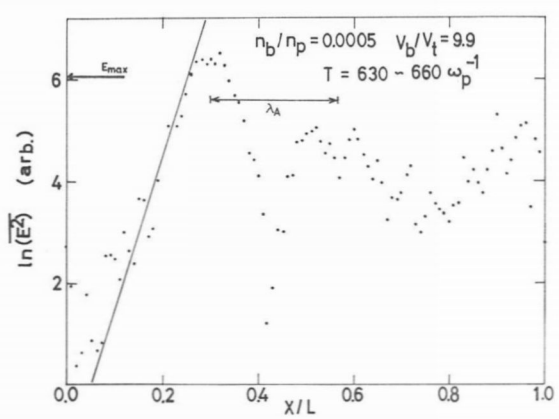

FIG. 7. The spatial dependence of the average wave power between $t = 630\ \omega_p^{-1}$ and $660\ \omega_p^{-1}$ (run E3).

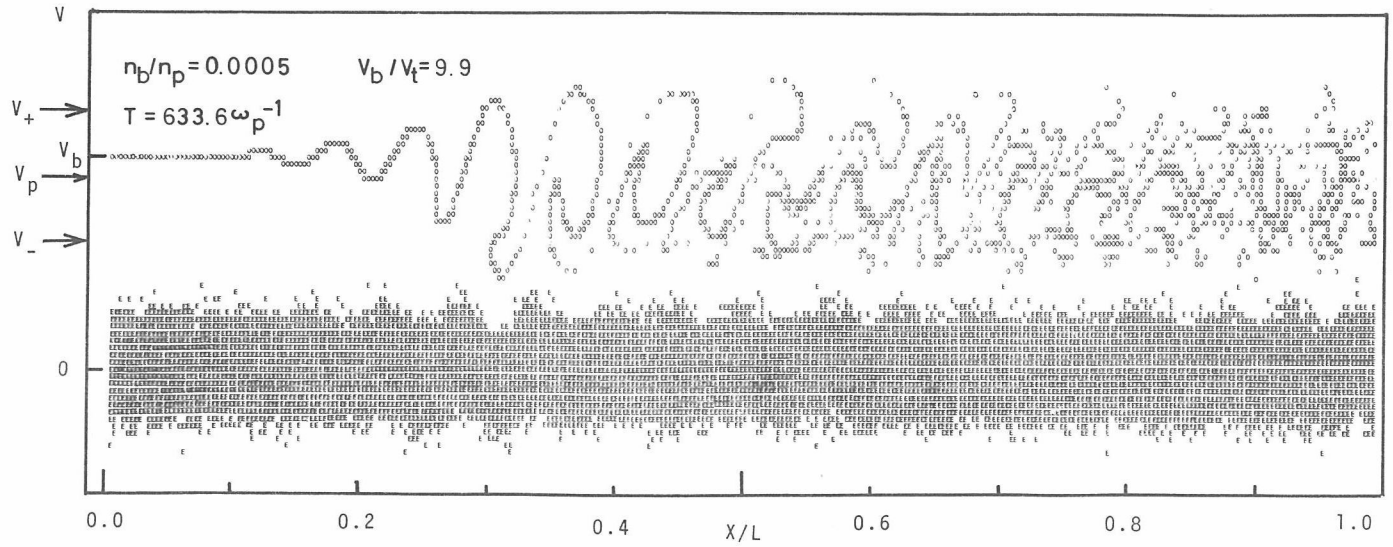

FIG. 8. The instantaneous phase space plot at the time corresponding to that in Fig. 7 (run E3).

Next, we examined the corresponding evolution of the beam electrons in the slightly collisional case for reconfirmation of these conclusions. In Fig. 10, this evolution is summarized in the sequence of the phase space loci of the beam electrons at the characteristic positions denoted in Fig. 9. Each locus is composed of the phase space points of the 200 beam electrons, which are plotted at every two electrons. In accordance with amplitude oscillation, the sloshing back and forth of the trapped beam electrons in the wave trough appears. Al-

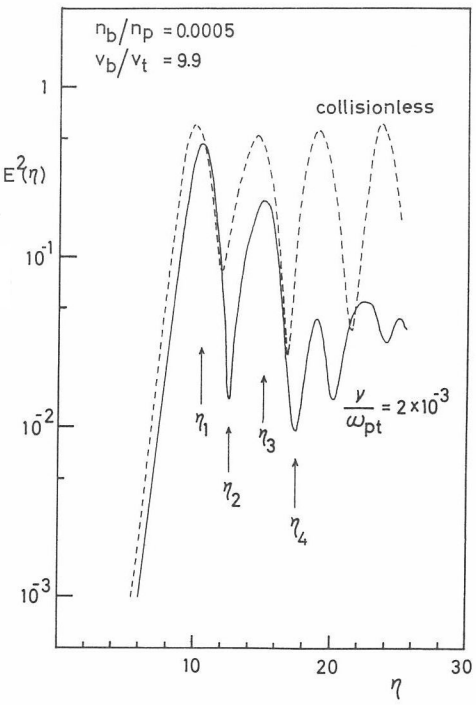

FIG. 9. Comparison of spatial dependences of the wave power between collisionless case (dashed curve) and the slightly collisional case (solid curve): $\nu/\omega_p = 2\times10^{-3}$, $\eta = \kappa k_0 x$ and the other plasma parameters are fit to those in run E3. These are numerically calculated from the extended single wave model equations.[11]

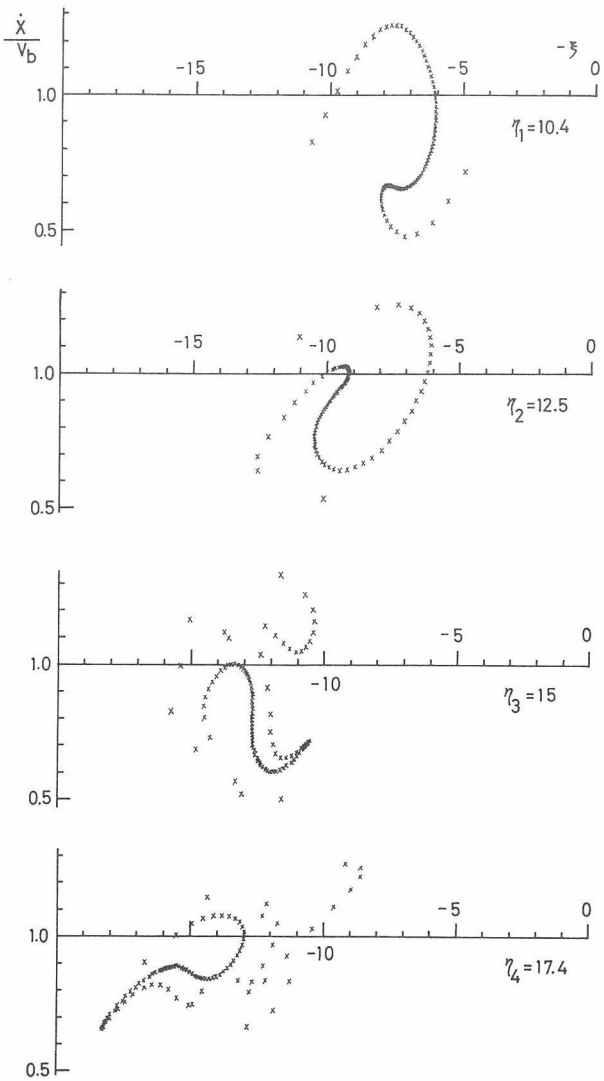

FIG. 10. Phase space loci for the beam electrons at the positions denoted in Fig. 9. Each point gives the normalized beam velocity $\dot{x}/v_b$ and a phase ξ_j of the jth beam electron, where ξ_j/ω_{pt} is a difference between the time when the beam electron reaches the position x and the time, x/v_b.[11]

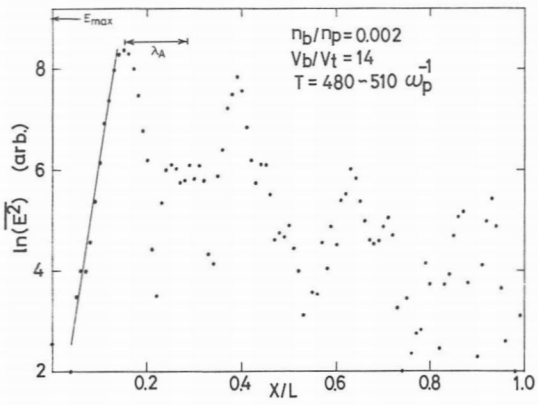

FIG. 11. The spatial dependence of the average wave power between $t = 480\ \omega_p^{-1}$ and $510\ \omega_p^{-1}$ for run E4.

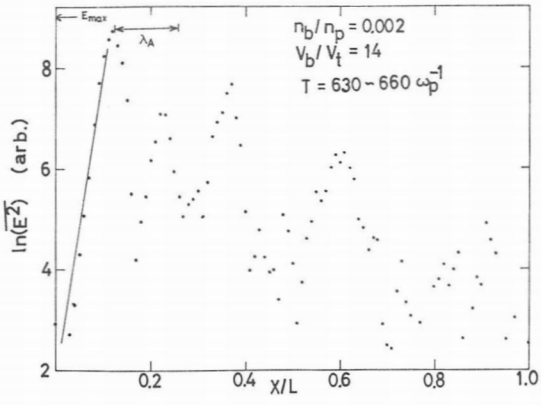

FIG. 13. The spatial dependence of the average wave power between $t = 630\ \omega_p^{-1}$ and $660\ \omega_p^{-1}$ in the final state (run E4).

though the motion of the beam electrons in phase space is still a reversible process in the earlier nonlinear stage, after saturation of the wave amplitude its behavior gradually changes from that of the collisionless case. Near the point η_3, the locus splits into two parts and forms a double vortex structure. Next, the vortices in phase space begin to be smeared out in an irreversible manner after η_4. These features are close to those in Fig. 8, and contrasted with those in the collisionless case, for which the numerical calculation of the usual single wave model equations[6] shows that the single vortex is persistent as the main phase space loci even at the second maximum of the electric field.

Run E4 has the largest expansion parameter of $\kappa = 0.4$ among the ones presented here. As shown later, the minimum velocity reaches zero in this case. When κ or the maximum wave amplitude is so large that the beam velocity reaches zero or changes its sign, the transformation of the variables introduced for derivation of the single wave model equations becomes inappropriate, because the differential equations of Eq. (3) in Ref. 11 become singular near zero beam velocity. In addition, the plasma electrons cannot be treated as a linear dielectric medium. Accordingly, its solution becomes invalid near $\kappa = 0.4$. In the usual particle simulation, we do not need such a transformation and assumptions. We can simulate the system, even if the beam velocity becomes negative instantaneously.

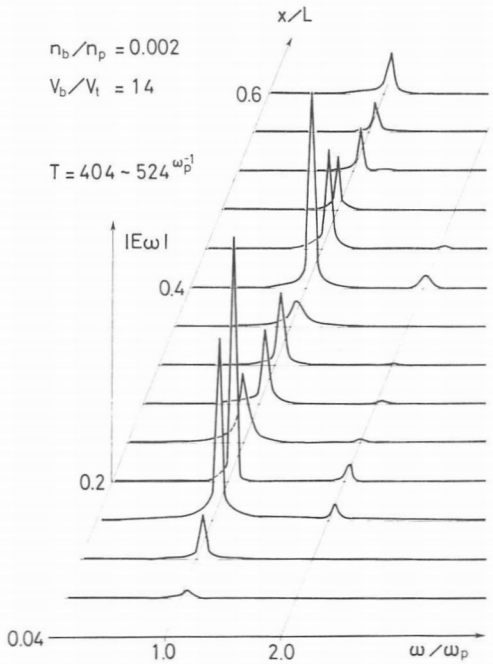

FIG. 12. The spatial dependence of the frequency spectra between $t = 404\ \omega_p^{-1}$ and $524\ \omega_p^{-1}$. The minimum frequency separation is $0.052\ \omega_p$ (run E4).

Figures 11 and 12 are spatial variations of the wave power and frequency spectra. Figure 12 shows that this wave is a coherent wave through the whole spatial evolution. As shown in Fig. 13, one more maximum grows after $150\ \omega_p^{-1}$ in the middle of the two maxima. As a result, three amplitude oscillations are clearly observed. Now, we can conclude that the persistent amplitude oscillation can exist in the large expansion parameter κ, in which the single wave model equations are invalid and the nonlinearities of the background electrons cannot be neglected. Figure 14 is the corresponding phase space plot. The velocity of the beam electron becomes zero at the maximum of the wave amplitude, which fairly well agree with $v_{b_{min}}$ calculated from Eqs. (10)–(12).

V. DISCUSSION AND CONCLUSIONS

The single wave model prediction[2,6] suggests that the properties of the nonlinearities in a small cold beam and plasma system are comparably simple among the nonlinear problems and that the basic equations are reduced to the unique scaled equations. In the usual parameters which have been treated in the experiments and simulations, it has been verified up to the region near the first minimum of the wave amplitude, however, after that region, it has disagreed with the results of experiments[13] and this simulation. Up to now, some mechanisms which destroy the regular amplitude oscillations of the electric field have been proposed by some authors. These are the weak collisions,[11,17] the nonlinearities of plasma oscillation in the background plasma,[7] and the trapped particle instability and the many wave effects associated with this instability.[10]

Here, we discuss the influence of these mechanisms on our results, comparing them with those of other simulations,[18,19] a theoretical and numerical work,[10] and the

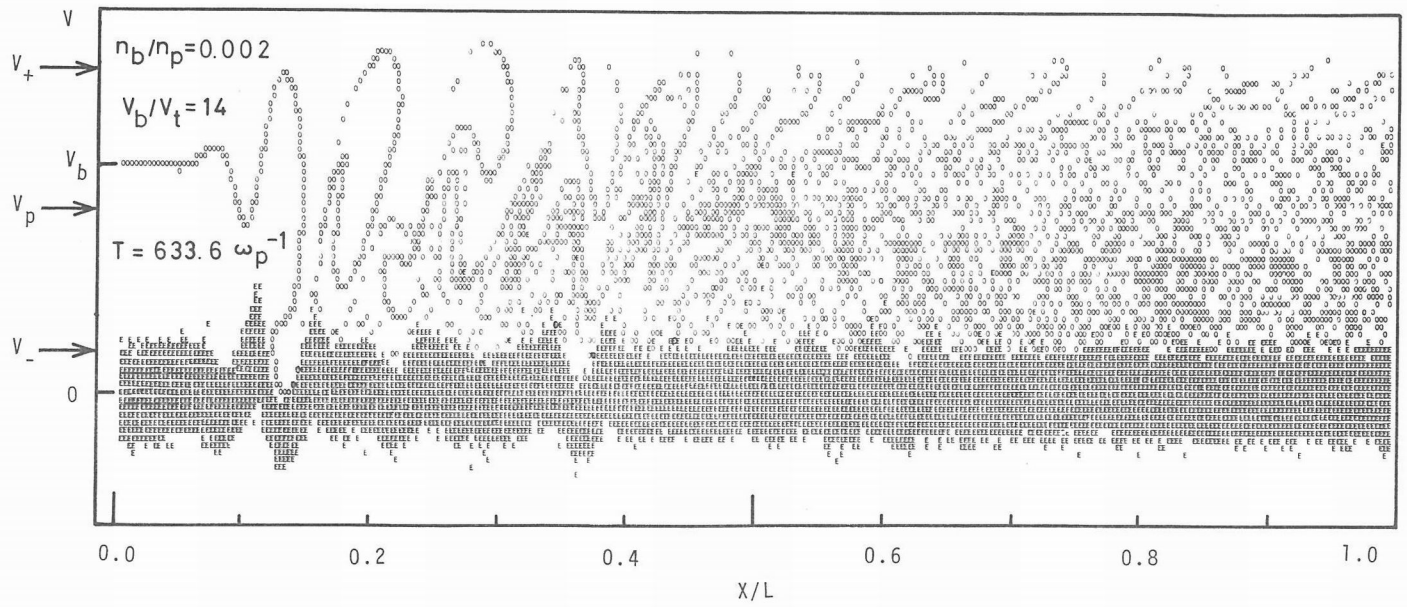

FIG. 14. The instantaneous phase space plot. Symbols O and E denote the positions in phase space for the beam electrons and background electrons, respectively. Some background electrons are observed to be accelerated to high velocity (run E4).

experiments.[14,26] Treating the temporal case by means of particle simulation, Kainer *et al.* concluded the following[19]: Two distinct regimes were identified. For denser beams ($n_b/n_p \geq 0.038$) it was observed that the rapid growth of the linearly most unstable wave led to merging of the beam distribution with the background distribution and the wave accelerated some main plasma electrons to high velocity causing it to drop back in amplitude. For the low density beam ($n_b/n_p \ll 0.038$) it was observed that after the initial growth of the most unstable mode and the accompanying spread in velocity, the beam decelerated and thermalized in quantitative agreement with the quasi-linear calculations.

Now, let us compare their results with our results. It was observed that the minimum amplitude of the wave and the phase space loci of the beam electrons were affected by the weak collision between the background electrons. These are the features which are not clear or not seen in the data in Refs. 18 and 19 which treat the temporal evolutions, although the background electrons in a Debye length used in their simulations were nearly equal to or less than those in our simulation.

For the larger expansion parameter of $\kappa = 0.4$, which corresponds to denser beams in the temporal case, we observed three amplitude oscillations, although the beam electrons were deeply merged with the background electrons and the wave accelerated some background electrons to high energy. This is also in contrast to the temporal case.[19] For the small expansion parameter $\kappa = 0.2$, it was observed that the regular amplitude oscillation was destroyed by the weak collision. In this work, there existed no regime where the quasi-linear theory could be applicable, because we did not reduce κ sufficiently due to the smallness of the available number of background electrons.

It could not be clarified in this work whether the nonlinearities of the background electrons[7] contribute to the destruction of the amplitude oscillation or not. However, the following facts were observed experimentally: In run E1, the destruction occurred just after the beam velocity distribution merged with the background distribution. However, the weak collision[11] or the trapped particle instability[10] can also be considered as a candidate for the origin of the destruction. On the other hand, the three amplitude oscillations have been observed in the parameter $\kappa = 0.4$, where the nonlinearities of the background plasma and the merging were strongest among the runs presented in this work. This problem remains unsolved, theoretically.

Recently, Winfrey and Dunlop[10] have extended the single wave model to the model of fifteen waves and studied the linear and nonlinear self-consistent evolution with the beam and a non-resonant plasma. They have concluded that the trapped particle instability occurs in a beam-plasma system with the larger expansion parameter κ and the mechanism of growth may be a secondary instability caused by the trapped electron distribution in the nonlinear beam. With these conclusions, we discuss this phenomenon concerning runs E1 and E4. The beam is trapped by the wave, and the average velocity of the beam decreases to the value near the phase velocity, therefore, the frequency of the secondary instability should be increased, as shown in Ref. 10. This phenomenon can occur long before the point of saturation of the wave amplitude. Following their model, we numerically calculated the examples of $v_b/v_t = 3.6$, 4.5 and $n_b/n_p = 10^{-3}$, 6.4×10^{-4} (both κ have the same value of 0.13) by the use of 600 beam electrons and five modes, whose frequencies were ω_{pt}, $\omega_{pt} \pm \Delta\omega$, $\omega_{pt} \pm 2\Delta\omega$ ($\Delta\omega = 0.01\ \omega_{pt}$). The calculations up to the point of the saturation of the wave amplitude showed that the linearly most unstable mode of the frequency ω_{pt} and the next upper two modes grew together and that the modes of the frequencies ω_{pt} and $\omega_{pt} + \Delta\omega$ were saturated near the point of the wave power less, by a factor of about 0.1, than the maximum which was predicted by O'Neill *et al.*[6] The mode of $\omega_{pt} + 2\Delta\omega$ was saturated near the point of the wave power

less, by a factor of about 2/3, than the maximum. This suggested that the frequency of the most dominant mode nonlinearly shifted to the upper side by more than 0.02 ω_p. Winfrey and Dunlop[10] summarized this trend in the temporal cases: Essentially, one wave dominates the others for most times. For large beams, the largest nonlinear wave resembles the single wave model prediction somewhat but occurs at a nonlinearly shifted wavenumber. Now, we can conclude that this phenomenon is related to the observation that the frequency of the most dominant mode in run E1 was larger by about 0.03 ω_p, although the poor frequency resolution of the wave spectra in run E1 prevented us from a detailed analysis.

Next, we observed a clear frequency shift of about 5% to the still higher side at the point of the minimum electric field with the destruction of the amplitude oscillation after the minimum in run E1. However, this frequency shift might be mainly due to the overdamping of the most dominant mode rather than due to the growth of the side band mode, as shown in Fig. 4(b). The amplitudes of the side band modes varied as that of the most dominant mode up to the point of the minimum of the wave amplitude. This behavior does not necessarily correspond to the results in Ref. 10.

The amplitude oscillation observed in run E4 which had a large expansion parameter cannot be predicted from the results of Ref. 10. One of the causes may be attributed to the differences in the plasma parameters between these runs and the runs adopted in their work, and to the collisional effect which was not considered in their work. These problems have remained unresolved. A part of them will be resolved in the near future.

In this work, we have suggested that the weak effective collisions of order, $\nu/\omega_p \sim 10^{-3}$, which are too small to alter the properties in the linear stage of the beam-plasma interactions, cause overdamping of the minimum amplitude, the associated destruction of the amplitude oscillation, and modification of the phase space loci of the beam electrons.[11] As an effective collision frequency ν, we can adopt one associated with the Coulomb collisions in dense plasmas. In addition, it has been suggested that, even when the Coulomb collision is negligible, some weakly nonlinear process (like parametric instabilities) may correspond to the effective collision.[8,17] At the present time, however, we cannot self-consistently estimate the magnitude of their exact effective collision which may change as the wave amplitude. This is a new problem to be considered in a future simulation where the ion is assumed to have finite mass or to be mobile. Therefore, let us restrict our considerations to Coulomb collisions. The effective collision frequency ν determines the damping of the plasma oscillation in the case of no beam[26] or is expressed as Eq. (1) in Ref. 11 for the plasma dielectric function $\epsilon(\omega, k)$

$$\epsilon(\omega, k) = 1 - \frac{\omega_p^2}{\omega(\omega + i\nu)}\left(1 + 3\frac{k^2 v_t^2}{\omega^2}\right). \tag{13}$$

Here, we should notice the features of the collision associated with a one-species, one-dimensional plasma corresponding to the background electrons. Dawson[25] confirmed experimentally that the relaxation time for thermalization was proportional to $(n_p\lambda_D)^2$ and pointed out that it was not caused by two-particle collisions, i.e., by including only two-particle correlations which vanish in such a plasma, but by three-particle correlations.

The damping of plasma oscillation due to only Coulomb collision has been discussed by some authors.[26-28] Shkarofsky[27] and McBride[28] calculated the damping rate using the Fokker–Planck equation and moment equation approach and obtained a formula

$$\nu/\omega_p = \left(\frac{2}{\pi}\right)^{1/2}\frac{\ln\Lambda}{\Lambda}\left[1 - \left(2 - \frac{4\times 2^{1/2}}{5}\right)(k\lambda_D)^2\right], \tag{14}$$

where $\Lambda = 12\pi n_p \lambda_D^3$. According to this formula, the anomalous collisional effects presented here might be neglected in the experiment by Gentle and Lohr,[14] because their plasma was tenuous where ν/ω_p might be less than 10^{-5}. On the other hand, Böhmer *et al.*[26] studied the influence of collisions on the instability in the beam and dense plasma mainly in the linear stage, both theoretically and experimentally. They used the background plasma, whose plasma densities were between 1.5×10^{13} and 2×10^{11} cm^{-3} and whose plasma temperatures varied between 900° and room temperature. In this plasma, the magnitude of the collision became larger than of the order of $\nu/\omega_p \sim 10^{-2}$. Therefore, the phenomena associated with the weak collision should be observed in the appropriate plasma parameters. Actually, Fig. 7 in their paper[26] showed an anomalous decay of the wave amplitude after its saturation, although whole the plasma parameters were not presented and so direct comparison is impossible. As the origin of the decay, they proposed the self-quenching mechanism. It was a linear mechanism associated with the combined effects of the collision and the velocity spread of the beam after wave amplitude saturation. This self-quenching mechanism, perhaps, is independent of overdamping in the first minimum of the wave amplitude discussed in this paper, but may be related to the destruction of the subsequent amplitude oscillation. This is a future problem.

ACKNOWLEDGMENTS

The authors thank Professor H. Momota at the Institute of Plasma Physics at Nagoya University for stimulating discussions. They are also grateful to Dr. M. Tanaka of Japan Atomic Energy Research Institute for his useful discussions and encouragements. The numerical computations were performed at the Data Processing Center of Kyoto University.

[1]W. E. Drummond, J. H. Malmberg, T. M. O'Neil, and J. R. Thompson, Phys. Fluids **13**, 2422 (1970).
[2]T. M. O'Neil, J. H. Winfrey, and J. H. Malmberg, Phys. Fluids **14**, 1204 (1971).
[3]I. N. Onishchenko, A. R. Linetskii, N. G. Matsiborko, V. D. Shapiro, and V. I. Shevchenko, Zh. Eksp. Teor. Fiz. Pis'ma Red. **12**, 407 (1970) [JETP Lett. **12**, 281 (1970)].
[4]N. G. Matsiborko, I. N. Onishchenko, V. D. Shapiro, and V. I. Shevchenko, Plasma Phys. **14**, 591 (1972).
[5]J. R. Thompson, Phys. Fluids **14**, 1532 (1971).

[6]T. M. O'Neil and J. H. Winfrey, Phys. Fluids **15**, 1514(1972).
[7]V. D. Shapiro and V. I. Shevchenko, Nucl. Fusion **12**, 133 (1972).
[8]K. Jungwirth and L. Krlin, Plasma Phys. **17**, 861 (1975).
[9]K. Jungwirth, J. Plasma Phys. **13**, 1 (1975).
[10]J. H. Winfrey and M. L. Dunlop, Plasma Phys. **19**, 901 (1977).
[11]O. Fukumasa, H. Abe, and R. Itatani, Phys. Rev. Lett. **40**, 393 (1978).
[12]J. H. Malmberg and C. B. Wharton, Phys. Fluids **12**, 2600 (1969).
[13]K. W. Gentle and J. Lohr, Phys. Fluids **14**, 2780 (1971).
[14]K. W. Gentle and J. Lohr, Phys. Fluids **14**, 2780 (1971); or K. W. Gentle and J. Lohr, Phys. Rev. Lett. **30**, 75 (1973).
[15]K. Mizuno and S. Tanaka, J. Phys. Soc. Jpn. **35**, 1753 (1973); or K. Mizuno and S. Tanaka, Phys. Rev. Lett. **29**, 45 (1972).
[16]W. Carr, D. Boyd, R. Jones, and M. Seidel, Plasma Phys. **15**, 826 (1973).
[17]G. Dimonte and J. H. Malmberg, Phys. Rev. Lett. **38**, 401 (1977).
[18]V. T. Astrelin, N. S. Buchel'nikova, and Yu. P. Zakharov, Zh. Tekh. Fiz. **45**, 1184 (1975) [Sov. Phys.-Tech. Phys. **20**, 741 (1975)].
[19]S. Kainer, J. M. Dawson, R. Shanny, and T. Coffey, Phys. Fluids **15**, 493 (1972).
[20]H. Naitou and H. Abe, Kakuyugo Kenkyu Suppl. **35**, 63 (1976) (circular in Japanese).
[21]H. Abe, R. Itatani, and H. Momota (to be published).
[22]C. K. Birdsall, A. B. Langdon, and H. Okuda, in *Methods in Computational Physics*, edited by B. Alder, S. Fernbach, and M. Rotenberg (Academic, New York, 1970), Vol. 9, p. 241.
[23]H. Abe, J. Miyamoto, and R. Itatani, J. Comput. Phys. **19**, 134 (1975).
[24]H. R. Lewis, A. Sykes, and J. A. Wesson, J. Comput. Phys. **10**, 85 (1972).
[25]J. M. Dawson, Phys. Fluids **7**, 419 (1964).
[26]H. Böhmer, J. Chang, and M. Raether, Phys. Fluids **14**, 150 (1971).
[27]I. P. Shkarofsky, Phys. Fluids **11**, 2454 (1968).
[28]J. B. McBride, Phys. Fluids **12**, 844 (1969).